Observations of the micro-structure of a radar bright band and associated shower[1]

By EDWARD N. BROWN,[2] *University of Chicago, Department of Geophysical Sciences*

(Manuscript received June 29, 1964)

ABSTRACT

Observations on a micro-structure scale were obtained of a radar bright band. The most important interpretations of the observations indicate: (1) Snow pellet aggregation occurs above and in the upper band levels, (2) Thermodynamically, the band is identified by an isothermal layer and a thin unstable layer (2.30°C/100 meters) near the band base.

1. Introduction

The bright band or bright line, an extremely pronounced horizontal echo observed with weather radars, is generally attributed to the melting of snow pellets or crystals as they descend below the 0°C level. This phenomenon has been studied theoretically by RYDE (1946) and WEXLER (1955) and others, and examined to some extent with meteorological measurements by HOOPER & KIPPAX (1950), AUSTIN & BEMIS (1950) and BYERS & COONS (1947). There also have been several investigations which combined radar with other instrumentation to obtain empirical data about this phenomenon. Particularly relevant is the work of HOOPER & KIPPAX (1950) who obtained simultaneous radiosonde and radar measurements and that of CUNNINGHAM (1947) who examined several bright band phenomena with an instrumented aircraft.

During the 1962 Project Whitetop field program in Southern Missouri several cloud regimes displaying prominent radar bright band phenomena were examined. Simultaneous radar observations (vertical scan APS-10), dry bulb temperature, liquid-water content and precipitation particle measurements were obtained at levels above, in, and below the bright band. One set of these data has been reduced and an observation interpretation is presented since this represents a preliminary step in examining the micro-structure of a radar bright band in meteorological detail. The measurements were obtained with a Beech D-18 aircraft instrumented for atmospheric research by Project Whitetop, Department of Geophysical Sciences, University of Chicago.

[1] The research reported in this article has been sponsored by the National Science Foundation under Grant G-22419.

[2] Now associated with the National Center for Atmospheric Research, Boulder, Colorado.

2. Observational data

2.1. Cloud conditions

The attending cloud system consisted of three distinct types as reconstructed from aircraft and ground observations:

(1) Lower stratocumulus, about 2000 ft thick, with base altitude of 5000 or 6000 ft mean sea level.
(2) A middle layer of altostratus with base estimated about 15,000 ft which contained nodules or convective turrets of about 3000 ft in depth—this cloud layer was not extensive but rather broken and patchy.
(3) A high cirrus overcast very roughly estimated to be at 20,000 ft.

The slant visibility, particularly at higher levels, was judged "murky" which leaves doubt as to whether a small particle cloud existed in addition to the larger snow pellets which were collected in and above the band top. It is often difficult to determine visually when the aircraft is in cloud when flying between layer clouds. The interpretation is marginal but it seems

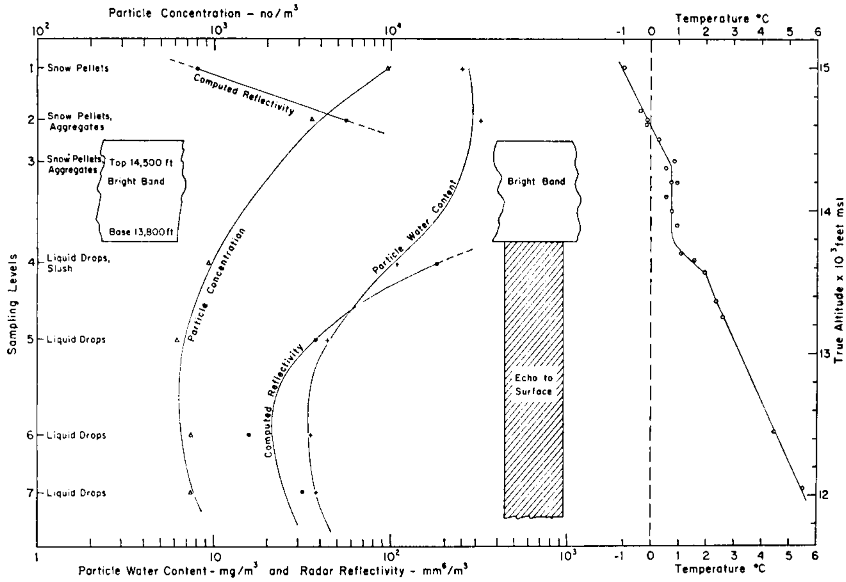

FIG. 1. Vertical cross section of a radar bright band. The parameters of particle concentration, computed precipitation water content and radar reflectivity were determined from precipitation particle measurements at the various levels. Temperature, measured with a reverse flow platinum wire sensor, is corrected for dynamic heating and pressure altitude is corrected to true altitude. In positioning the bright band radar pulse-length effects have been neglected. The segment of the reflectivity profile between levels 2 and 4 could not be determined.

likely that the bright band was associated only with the precipitation from the altostratus layer since the liquid-water measurements are not suggestive of data generally obtained from clouds which contain any significant amount of water as droplets. This does not imply that solid hydrometeors, too small to be detected, were not present.

2.2. Flight procedure

The flight procedure consisted of a series of descending steps beginning above and terminating below the radar band. At each level measurements were obtained for a period of 45–60 seconds. Since the horizontal extent of the band was limited an effort was made to align the successive passes of the aircraft with respect to the most intense part of the band at each level and to adjust the over-all descent rate according to the estimated fall speed of the particles. The over-all descent rate was adjusted to about 3 ft/sec. The former requirement was more difficult to achieve since the band could not be detected visually. Procedure turns and radar vectoring were used for fixing the track for the measurement period at each level. The resultant tracks were parallel but not precisely vertically aligned. The mean track separation from the band mid-point was about 2000 meters except for the level 3 track which intercepted the band edge.

2.3. Radar observations

Radar observations were made with a vertical scanning, 3 cm APS-10. Fig. 2 illustrates the radar band and shower structure corresponding in time to the measurements at level 2 (A) and level 4 (B). At the outset (level 1, time 0) the band was 3–4 miles across and the top and base were sharp and well defined. About the time of the level 2 measurements the base of the band became irregular near the midpoint and during passes at levels 5, 6 and 7 the base of the band was obscured by echo from a drizzle shower. At this time the shower was 3–4 miles wide or about the same horizontal extent as the band at level 1. Although the precipitation was light, as suggested by the drop distributions of Table 1, it was detected by a recording rain gage on the surface.

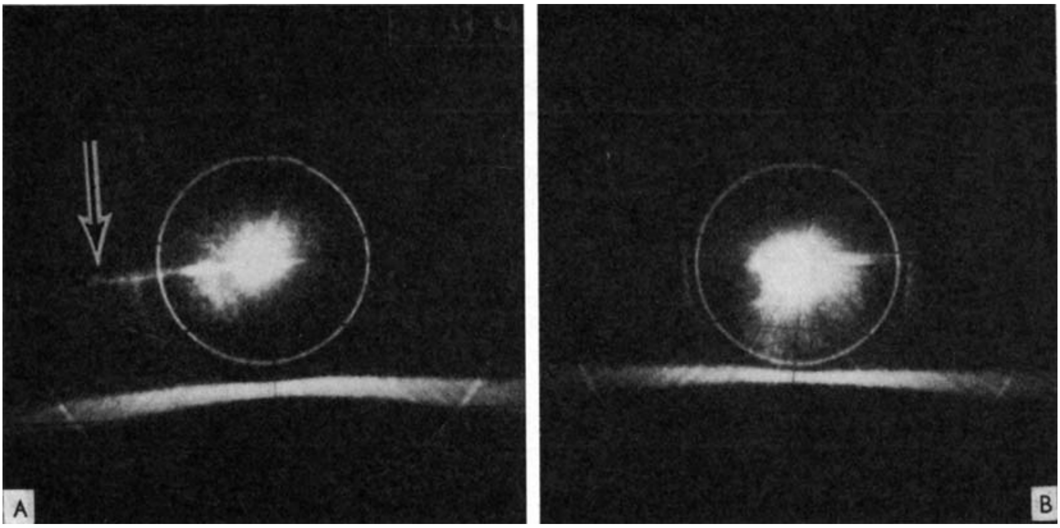

FIG. 2. The bright band structure corresponding in time to the measurements at level 2 (A), and at level 4 (B). The rain shower beneath the band reaches the surface in Photo B. Range markers are 2 nautical mile intervals.

The height of the band was determined by a range marker-true altitude calibration. In the range of 2–3 miles there is reasonable agreement between these values. The major source of position error results from radar film reading inaccuracies and pulse-length effects. Position error introduced by film reading is conservatively estimated to be ± 100 ft. It is recognized the pulse-length effect on range distortion is considerably larger ($h/2$) or about 200–300 ft for the APS-10 radar. Range distortion correction has not been applied to the band position shown in Fig. 1.

2.4. Snow pellet and drop measurements

The particle distributions were obtained with a foil sampler device and are shown in Table 1. The evaluation of the particle measurements for the lower four levels follows the foil calibration by Brown (1958, 1961). The foil sensor has not been calibrated for solid particle impaction (viz., snow pellets found at levels 1, 2 and 3) but these impressions can be readily distinguished from those resulting from either liquid drops or fragile, low-density snow flakes. In terms of sizing the pellets, the impression diameter is considered to be the particle diameter.

Radar reflectivity values shown in Fig. 1 for the particle distributions of Table 1 were computed using $|K|^2$ values of 0.19 and 0.93 [Battan (1959)] respectively for snow pellets and liquid drops of the appropriate levels.

The observations indicate that the particles were solid at the upper levels. A very high concentration of 200–500 μ diameter pellets were measured at level 1 above the band. The foil sampler records show aggregates of particles at levels 2 and 3 and we found the spectrum broadened to include the 1 mm diameter aggregates while the concentration of the smaller pellets decreased. The aggregates at level 2, about the top of the band, consisted of 5–10 smaller pellets. The observations at level 3 also showed evidence of particle aggregation but the distribution was not considered representative since the flight track had intercepted the edge of the band.

Particle measurements in the drizzle shower slightly below the band (level 4) indicate that all particles were liquid except those larger than 950 microns diameter. At level 5 and below, particle distributions were essentially the same as is shown in Fig. 1 by constant values of concentration, computed liquid-water content, and radar reflectivity.

TABLE 1. *Concentrations (number per cubic meter) of hydrometeors at various levels above and below a bright band.*

The values have been averaged from measurements along a $1\frac{1}{2}$ mile track at each level.

Level	Time sec	Particle composition	*Particle diameter*, in tens of microns 20–30	30–40	40–50	50–60	60–70	70–80	80–90	Aggregates > 100
1	0	Snow pellets	2311	3193	3877	267	0	0	0	0
2	187	Snow pellets and aggregates	134	651	296	905	920	292	13	60
3	351	Snow pellets and aggregates	On band edge—did not evaluate							
			Drop diameter, in tens of microns 25–35	35–45	45–55	55–65	65–75	75–85	85–95	> 95
4	506	Water drops and slush	321	271	110	68	60	44	2	57
5	669	Water drops	230	165	94	28	36	26	8	8
6	860	Water drops	394	181	94	21	43	13	9	0
7	1034	Water drops	448	143	73	28	30	17	15	4

2.5. STATIC TEMPERATURE MEASUREMENTS

A measure of the air temperature was obtained with a platinum resistance element in a non-wetting, reverse flow housing. The measured temperatures were corrected for dynamic heating ($r = 0.64$). The free air or static temperatures plotted in Fig. 1 are averages of values measured at 4 to 6 individual points at each level.

Above the band and extending 200 feet below the band top, and beginning 200 ft below the band base and extending downward for another 2000 ft the temperature lapse rate was about 0.8°C/100 meters or intermediate between the dry and wet adiabatic rates for these levels. From a point about 200 ft below the band top and extending downward to 13,700–13,800 ft, the level of the projected base, the lapse rate was isothermal at a temperature of +0.6 to +0.7°C. Immediately below the base (in the drizzle shower) we found an unstable layer about 40 meters deep where the lapse rate was 2.30°C/100 meters.

It would be desirable in this study to be able to accept these temperatures as absolute values. However this is not too advisable since the estimate of total error (±0.5°C) is sufficient to invalidate much of the temperature structure. On the other hand the isothermal layer and the unstable layer below the band have both been predicted in theoretical analyses.

3. Interpretation of observations

The variety and accuracy of data necessary for a complete analysis of a transient, micro-scale radar phenomenon such as the bright band places great demands upon an instrument system and in many cases requires measurements which are difficult to obtain directly. Inherent instrument errors and the unmeasured pellet and vapor densities turn out to be very important factors in this case. By considering the basic observations previously outlined, the following interpretations are offered as a partial description of the processes going on within this bright band and associated shower:

(*a*) Considering position accuracy, the top of the band was about the 0°C level.

(*b*) The aggregation of pellets which was observed to be going on above and in the upper band levels played a large role in determining the top of the band.

(*c*) If we accept the isothermal layer as identifying the layer being cooled by melting pellets, the data suggest that very little melting was taking place in the upper 200 ft of the band. Also, the particle measurements below the projected horizontal base of the band indicated that the large particles were not completely melted after descending the depth of the band.

(*d*) The observation of an unstable layer (2.30°C/100 meters) is further evidence of a turbulent zone just below the band as suggested by ROGERS (1957) and WEXLER (1957).

(*e*) As noted, a direct measurement of pellet density was not possible under the circumstances but it is practical through an analysis of radar reflectivity to determine an approximate "transfer function" from which the pellet density can be estimated. The observation of echo around the aircraft and out to 1–2 mile range while at levels 5, 6 and 7 (particles known to be liquid and $|K|^2$ is established) means that the threshold reflectivity of the radar at the time corresponded to a Z-value of 20–40 mm^6/m^3 at these levels. Performance based upon calibration data for the APS-10 suggests respective reflectivity thresholds of 20–90 mm^6/m^3 for the 1 and 2 mile range. Since these values straddle the reflectivity values computed from the distributions for levels 5, 6 and 7 it is concluded the radar was operating according to normal characteristics. Even with the knowledge of the particle distribution at levels 1 and 2, the $|K|^2Z$ values are somewhat uncertain because of the unknown pellet density which influences the value of $|K|^2$. ATLAS *et al.* (1953) have shown the effective value of K for an air-ice particle to be:

$$K_p = \frac{\varrho_p}{\varrho_i} K_i,$$

where subscript p refers to the pellet and ϱ_i is the density of ice. Thus effective $|K_p|^2Z$ values for various pellet densities can be computed. These are listed, for levels 1 and 2, in Table 2.

With the assurance that the APS-10 was operating normally, an echo would not be expected at level 1 regardless of the densities of the pellets. At level 2, very near the bright band top, the computed values of $|K_p|^2Z$ correspond to nominal threshold values only for a high density pellet (0.6–0.9 gm/cm^3). Values reported in the literature range from 0.125 gm/cm^3, NAKAYA & TERADA (1935) for pellets falling from winter stratus, to more than 0.85 gm/cm^3 for pellets found just above the 0°C isotherm inside cumulus clouds, BRAHAM (1963). By considering the possibility that the band resulted from the precipitation of a convective turret observed above the altostratus and that a distinct detection threshold established by calibration is known for the foil impaction device, BROWN (1958, 1961), the author tends to favor a rather high density for the pellets. The computed values of water content for levels 1 and 2 assume a pellet density of 0.85 gm/cm^3.

(*f*) The reflectivity profile within the band could not be determined directly from the radar or particle measurements. Determination of the profile is complicated by the lack of reliable humidity data, the possibility of a non-steady state and the inexactness of estimating the particle distribution changes due to coalescence. At best, Fig. 1 shows the computed reflectivity values $|K_p|^2Z$ above the band (ϱ_p = 0.85 gm/cm^3) and in the drizzle shower below. The striking increase of reflectivity near the top of the band is *attributed to coalescence* since effective melting had not occurred at these levels.

Neglecting particle shape and orientation effects but considering the melting effect on scattering, the reflectivity profile within the band will reach a maximum between level 3 and 4. WEXLER (1957) postulates that as the cooling of the air by melting proceeds, the top portion of the layer is cooled to 0°C and the effective melting layer begins to shift downward and encroach upon the warmer air below. The lowering of the melting level thus would cause a corresponding downward shift of the maximum reflectivity of the band. Taking the isothermal temperature to be within a few tenths of 0°C would suggest the maximum reflectivity to be located in the extreme lower band levels where melting was occurring.

TABLE 2. *Radar reflectivities (mm^6/m^3) for levels 1 and 2 for pellet densities of 0.2–0.9 gm/cm^3.*

Density	$\lvert K_p\rvert^2/Z$ Level 1	Level 2
0.2	0.45	3.12
0.3	1.00	7.00
0.4	1.80	12.50
0.5	2.80	19.50
0.6	4.04	28.20
0.7	5.47	38.10
0.8	7.15	49.90
0.9	9.17	63.80

Summary

The bright-band phenomena described in this paper apparently formed from the aggregation of many small pellets into fewer large ones just above the zero centigrade level. This was followed by melting which, for the larger particles, extended throughout the depth of the band. The base of the band was not sharp and distinct but merged gradually into an echo from a drizzle shower (at least when seen from

a radar at very close range). Thus this situation appears rather unlike the typical bright band in which the band top is attributed only to the development of a water "skin" on low density snowflakes, and which has a sharp lower boundary attributed to the divergence of the raindrops as a result of increased fall speeds following melting. In this case the uncertainty of particle densities and the non-representativeness of the sample at level 3 makes it difficult to draw any conclusions concerning the divergence of the smaller particles following melting. However, in terms of the radar reflectivity it is the large particles that are important. We noted that these were not completely melted at level 4. If we accept the decrease in the measured concentration of these particles between levels 4 and 5 as due to particle divergence following melting we are forced to question our estimate of a high pellet density or alternatively to suggest that the particles increased speed and diverged not so much because of a density change but because of changes in the drag coefficient associated with changes in surface roughness. A similar result was suggested by WILLIS (1963) to explain certain experiments with falling ice spheres.

Acknowledgements

The author wishes to express his appreciation to Dr. Roscoe R. Braham, Jr., for his guidance and manuscript review, and to Mr. Arthur Bardige who assisted in data reduction.

REFERENCES

ATLAS, D., KERKER, M., and HITSCHFELD, W., 1953, Scattering and attenuation by non-spherical atmospheric particles. *J. Atmos. Terr. Phys.*, **3**, pp. 108–119.

AUSTIN, P. M., and BEMIS, A. C., 1950, A quantitative study of the bright band in radar precipitation studies. *J. Meteor.*, **7**, pp. 145–151.

BATTAN, L. J., 1959, *Radar Meteorology*, U. Chicago Press.

BRAHAM, R. R., JR., 1963, Some measurements of snow pellet densities. *J. Applied Meteor.*, **2**, pp. 498–500.

BROWN, E. N., 1958, A technique for measuring precipitation from aircraft. *J. Meteor.*, **15**, pp. 462–466.

BROWN, E. N., 1961, A continuous recording precipitation particle sampler. *J. Meteor.*, **18**, pp. 815–818.

BYERS, H. R., and COONS, R. D., 1947, The bright band in radar echoes and its probable explanation. *J. Meteor.*, **4**, pp. 75–81.

CUNNINGHAM, R. M., 1947, A different explanation of the bright band. *J. Meteor.*, **4**, p. 163.

HOOPER, J. E. N., and KIPPAX, A. A., 1950, The bright band—a phenomenon associated with radar echoes from falling rain. *Quart. J. R. Meteor. Soc.*, **76**, p. 125.

NAKAYA, U., and TERADA, T., 1935, Simultaneous observations of the mass, falling speed, and form of individual snow crystal. *J. Fac. Sci. Hokkaido, sec.* II, *Phy.*, **1**, pp. 169–171.

ROGERS, R., 1957, Radar measurements of gustiness. *Proc. 6th Weather Radar Conference.* American Meteorological Society, Boston, Mass., pp. 99–106.

RYDE, J. W., 1946, The attenuation and radar echoes produced at centimeter wave-lengths by various meteorological phenomena. Meteorological factors in radio wave propagation. *Physical Society and Royal Meteorological Society*, **169**.

WEXLER, R., 1955, The melting layer. Blue Hill Met. Obs., Harvard University, *Meteor. Radar Studies*, No. 3.

WEXLER, R., 1957, Advection and the melting layer. Blue Hill Met. Obs., Harvard University, *Meteor. Radar Studies*, No. 4.

WILLIS, J. T., BROWNING, K. A., and ATLAS, D., 1963, Radar observations of melting ice spheres. *Proc. 10th Weather Radar Conference*, American Meteorological Society, Washington, D.C., pp. 151–156.